Theory of Chaos in Surface Waves: The Reduction from Hydrodynamics to Few-Dimensional Dynamics

Ehud Meron and Itamar Procaccia

Department of Chemical Physics, The Weizmann Institute of Science, Rehovot 76100, Israel, and The James Franck Institute and the Department of Chemistry, University of Chicago, Chicago, Illinois 60637

(Received 19 August 1985)

The experiment on chaos in surface waves reported by Ciliberto and Gollub is used as a case model for an understanding of the appearance of few-dimensional chaos in systems with an infinite number of degrees of freedom. Center-manifold and normal-form theories are utilized to derive the pertinent dynamical system and to provide an approximate solution of the partial differential equations. Comparisons of theory and experiment are discussed.

PACS numbers: 05.45.+b

The recent effort in experimental research concerning the onset of chaos in hydrodynamic systems firmly established the fact that chaos sets in as a few-dimensional phenomenon even in systems that are traditionally described by partial differential equations (pde's).[1] The use of a small number of ordinary differential equations (ode's) (or maps thereof) to model the transition to chaos in hydrodynamics has thus been phenomenologically justified. What has been lacking so far, however, is an example where detailed theory and detailed experiment exist in parallel, so as to demonstrate how the tremendous reduction from an infinite to a finite number of degrees of freedom occurs in practice.[2] The aim of this Letter is to report on such a case.

As a case model we chose the experiment on chaos in surface waves reported by Ciliberto and Gollub.[3] Besides being an extremely detailed study with extensive results, this experiment is unique so far in the sense that the transition to chaos appears essentially directly from the quiescent state in a region of the phase diagram. This allows a development of the theory around the quiescent state in contrast with all other cases where a series of bifurcations, leading to a time-space–dependent state, precedes the onset of chaos. The case chosen here allows us to use the formalism suggested by Coullet and Spiegel[4] which utilizes the center-manifold theorem and normal-form theory to reduce the dynamics to a set of ode's.[5]

The experimental setup consists basically of a cylinder containing water which is mounted on a cone of a loudspeaker and is oscillated accurately in the vertical direction. When the amplitude of the oscillation exceeds some frequency-dependent threshold value, the free surface is deformed and surface modes appear. The modes are basically the eigenmodes of the operator $\nabla_\perp^2$, where $\nabla_\perp$ is $\partial_x\hat{\mathbf{x}}+\partial_y\hat{\mathbf{y}}$, and we conceive a Cartesian set of coordinates which moves with the cylinder such that the x-y plane is horizontal, and $z=0$ is at the free surface of the fluid in the quiescent state. These modes are $f_{l,m}\equiv J_l(k_{l,m}r)\sin(l\theta)$ or $J_l(k_{l,m}r)\cos(l\theta)$, where J_l is the Bessel function of order l, r is the radial coordinate, θ is the azimuthal coordinate, and the allowed wave numbers $k_{l,m}$ are determined by boundary conditions. In Fig. 1 we reproduce a portion of the experimental phase diagram in the region of parameter space where $f_{4,3}$ and $f_{7,2}$ appear to the excited modes. In the regions marked (4,3) and (7,2) the system displays these pure modes respectively, and they oscillate at one-half the driving frequency. For synchronization of the measurements at this frequency, Ref. 3 reported slow periodic oscillations and chaotic competition in the shaded region. The region of greatest interest to us is the vicinity of the point of intersection of the stability curves where it appears that the quiescent state might become chaotic with a small change of parameters. We develop the theory around this point.

It is noteworthy that a time-resolved Fourier analysis of the deformation field revealed many other modes with $l=3$, 8, 11, 14, 18, 21, 25, 28, etc. This seems at first perplexing when contrasted with the ex-

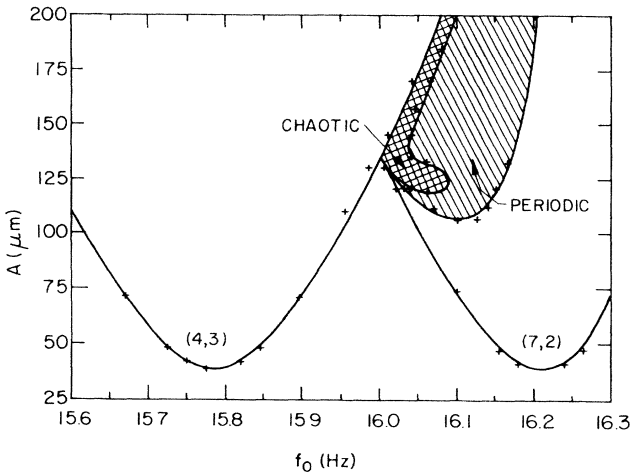

FIG. 1. Experimental phase diagram. The regions denoted (4,3) and (7,2) display single-mode patterns. In the shaded regions mode competition leads to slow-periodic and chaotic motions.

perimental determination of the dimension of the strange attractor which is smaller than 3. We shall see that our theory, which also yields an approximate solution of the pde's, rationalizes these findings.

The starting point of the theory is hydrodynamics. To simplify the algebra we neglect viscosity at first; one can obtain then a description of the dynamics with two scalar fields: the velocity potential $\phi(\mathbf{r},t)$ [where the velocity $\mathbf{v}(\mathbf{r},t)$ is $\nabla\phi(\mathbf{r},t)$] and the surface-deformation variable $z=\zeta(x,y,t)$. Following Benjamin and Ursell,[6] but supplementing nonlinear terms by expanding around $z=0$, we arrive at the following equations of motion in dimensionless units:

$$\partial\zeta/\partial t=\partial\phi/\partial z-N_1(\zeta,\phi), \tag{1a}$$

$$\frac{\partial\phi}{\partial t}=-\frac{1}{h\omega^2}\left(\frac{\gamma}{\rho h^2}\nabla_\perp^2-g+\tilde{A}\cos t\right)\zeta-N_2(\zeta,\phi), \tag{1b}$$

where γ, h, ω, ρ, g, and $\tilde{A}$ are the surface tension of the fluid, the depth of the fluid layer, the frequency of oscillation, the density of the fluid, the gravitational acceleration, and the amplitude of forcing, respectively. N_1 and N_2 are

$$N_1(\zeta,\phi)=\nabla_\perp\zeta\cdot\nabla_\perp\phi+\zeta\nabla_\perp^2\phi+\tfrac{1}{2}\zeta^2\nabla_\perp^2\,\partial\phi/\partial z+\zeta\nabla_\perp\zeta\cdot\nabla_\perp\,\partial\phi/\partial z+\ldots,$$

$$N_2=\tfrac{1}{2}|\nabla\phi|^2+\tfrac{1}{2}\zeta\,\partial(|\nabla\phi|^2)/\partial z+\ldots,$$

where the ellipsis represents higher-order terms. Some of the gross features of the phase diagram (Fig. 1) are obtained from the linearized theory, $N_1=N_2=0$. We picked the boundary conditions $\partial\phi/\partial n=0$ at the walls, $\partial\phi/\partial z=0$ at $z=h$ (the bottom of the cell), and $\partial\zeta/\partial n=0$ on the wall at the free surface (i.e., contact angle 90°; see below for discussion). Then, expanding ζ and ϕ in $f_{l,m}$ [i.e., $\zeta(x,y,t)=\sum_{l,m}\zeta_{l,m}(t)f_{l,m}(x,y)$, etc.], and denoting the amplitudes by a single index, ζ_l and ϕ_l, respectively, we arrive at a linear system:

$$\begin{pmatrix}\dot{\zeta}_l\\ \dot{\phi}_l\end{pmatrix}=\begin{pmatrix}0 & -\chi_l\\ \Gamma_l+\Lambda\cos t & 0\end{pmatrix}\begin{pmatrix}\zeta_l\\ \phi_l\end{pmatrix}\equiv\mathbf{K}_l\begin{pmatrix}\zeta_l\\ \phi_l\end{pmatrix}, \tag{2}$$

where $\chi_l=hk_l\tanh(hk_l)\sim O(1)$, $\Gamma_l=(1/h\omega^2)(\gamma k_l^2/\rho+g)\sim O(10^{-1})$, and $\Lambda=-\tilde{A}/h\omega^2\sim O(10^{-3})$. The numerical estimates pertain to the experimental conditions of Fig. 1. This system is a Floquet problem and is equivalent to the Mathieu equation

$$\ddot{\zeta}_l+(\omega_l^2+\chi_l\Lambda\cos t)\zeta=0, \tag{3}$$

where $\omega_l=\omega(\chi_l\Gamma_l)^{1/2}$ is the natural frequency of the l mode. Since Λ is so small we can find the neutral stability curves, which are the one-half tongues of the Mathieu equation, analytically via perturbation theory. The result takes the form

$$\Gamma_l(\Lambda)=1/4\chi_l\pm\tfrac{1}{2}\Lambda+O(\Lambda^2). \tag{4}$$

To compare with Fig. 1 we return to dimensional variables. In Fig. 2 we sketch the predictions of Eq. (4) as compared to the experimental situation. The modes $f_{4,3}$ and $f_{7,2}$ have neutral stability curves precisely in the right region of parameters. However, the mode $f_{11,1}$ which is not seen experimentally is found between them. The reason is the boundary condition $\partial\zeta/\partial n=0$. If we pick the condition $\zeta=0$ at the walls, the mode $f_{11,1}$ is pushed outside the region of interest, but the modes $f_{2,4}$ and $f_{10,1}$ creep in. Our conclusion is that the experimental boundary condition is neither, but a mixture of the two. We thus disregard the mode $f_{11,1}$ from now on.[7] Note that because of the neglect of damping the stability curves begin at $\Lambda=0$, but the point of intersection is right on the experimental frequency.

To proceed we want to use the center-manifold theorem[8] to reduce the dynamics to ode's, and normal-form theory[9] to obtain the simplest (minimal) nonlinear description. We thus expand the fields in the modes f_l, and, if we denote the amplitudes of $f_{4,3}$ and $f_{7,2}$ by α_l and the amplitudes of the rest of the modes by β_m, Eqs. (1) lead in principle to an infinite set of ode's:

$$\dot{\boldsymbol{\alpha}}_l=\mathbf{K}_l(t)\boldsymbol{\alpha}_l+\mathbf{g}_l(\{\boldsymbol{\alpha}_l\},\{\boldsymbol{\beta}_l\}), \tag{5a}$$

$$\dot{\boldsymbol{\beta}}_m=\mathbf{K}_m(t)\boldsymbol{\beta}_m+\mathbf{g}_m(\{\boldsymbol{\alpha}_l\},\{\boldsymbol{\beta}_l\}). \tag{5b}$$

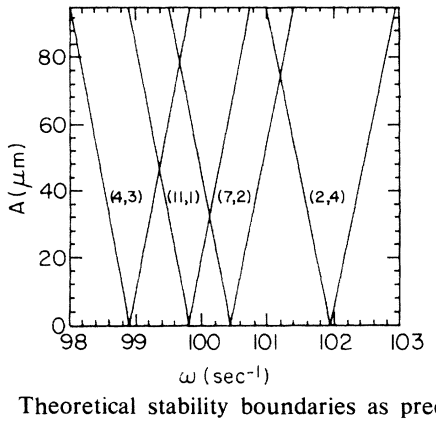

FIG. 2. Theoretical stability boundaries as predicted by the linearized theory without damping. The mode (10,1) has a tongue to the left of the mode (4,3). The ordinate is $A=2h|\Lambda|$.

Since these equations are not autonomous, the separation into stable and unstable modes should be based on a Floquet analysis. Since we neglected dissipation, there are no Floquet exponents with negative real part for the system (5). However, in the physical system dissipation exists, and near the point of intersection of the stability curves, only two such exponents cross the imaginary axis. Besides serving this important rule of separating stable from unstable modes, dissipation is not important as far as the normal form is concerned. We thus derive the normal form from (5), adding dissipation at the end. For this derivation we need autonomous equations.[4] To make (5) autonomous we introduce an artificial "critical" degree of freedom α_c, $\alpha_c \equiv \frac{1}{2}\Lambda e^{it}$, such that $\dot{\alpha}_c = i\alpha_c$ and $\dot{\alpha}_c^* = -i\alpha_c^*$. The cosine term in $\mathbf{K}(t)$ is then $\alpha_c + \alpha_c^*$. Accordingly the matrix $\mathbf{K}$ simplifies to

$$\mathbf{K}_i' = \begin{pmatrix} 0 & -\chi_i \\ \Gamma_i & 0 \end{pmatrix}$$

and the cosine term is pushed to the nonlinear $\mathbf{g}_i'(\{\alpha_l\},\{\beta_l\})$. It is noteworthy that in this form the linear problem near the point of intersection in Fig. 1 can be diagonalized to read $\dot{\tilde{\alpha}} = \mathbf{J}\tilde{\alpha}$, where

$$\mathbf{J} = \begin{pmatrix} i\Omega_{4,3} & & & & & & \\ & -i\Omega_{4,3} & & & & 0 & \\ & & i\Omega_{7,2} & & & & \\ & & & -i\Omega_{7,2} & & & \\ & 0 & & & i & & \\ & & & & & -i & \end{pmatrix}, \tag{6}$$

with $\Omega_l = \omega_l/\omega$. Thus the linear matrix at this point is technically similar to the one obtained for codimension-3 bifurcations. Accordingly, one might be less surprised that chaos can set in very close to this point.

The analysis from this point follows very closely the formalism proposed by Coullet and Spiegel.[4] After a considerable amount of algebra that will be reported elsewhere we find the following normal form:

$$\dot{\alpha}_a = (i\Omega_a - \lambda_a)\alpha_a + i\gamma_1 e^{it}\alpha_a^* + i\gamma_2|\alpha_a|^2\alpha_a + i\gamma_3|\alpha_b|^2\alpha_a + i\gamma_4\alpha_a^*\alpha_b^2, \tag{7a}$$

$$\dot{\alpha}_b = (i\Omega_b - \lambda_b)\alpha_b + i\delta_1 e^{it}\alpha_b^* + i\delta_2|\alpha_b|^2\alpha_b + i\delta_3|\alpha_a|^2\alpha_b + i\delta_4\alpha_b^*\alpha_a^2, \tag{7b}$$

where $a \equiv 4,3$ and $b \equiv 7,2$. We derived analytic expressions for the coefficients γ_i and δ_i and evaluated them numerically for the boundary conditions $\partial\zeta/\partial n = 0$. λ_a and λ_b are phenomenological. The theory also yields a solution for the fields. The most interesting is the deformation field $\zeta(x,y,t)$ which is found in the form

$$\zeta(x,y,t) = \zeta^{(1)}(x,y,t) + \zeta^{(2)}(x,y,t) + \zeta^{(3)}(x,y,t), \tag{8}$$

where

$$\zeta^{(1)}(x,y,t) = (i/\sqrt{2})\alpha_{4,3}f_{4,3} + (i/\sqrt{2})\alpha_{7,2}f_{7,2} + \text{c.c.},$$

whereas $\zeta^{(2)}(x,y,t)$ is quadratic in the amplitudes α and contains modes with $l = 0$, 3, 4, 7, 8, 11, and 14, and $\zeta^{(3)}(x,y,t)$ is cubic in α and contains modes with $l = 1$, 4, 7, 10, 12, 15, 18, and 21. All the time-dependent coefficients are known once Eqs. (7) are solved. One sees that to lowest order only $f_{4,3}$ and $f_{7,2}$ are expected to exist. However, to higher order the stable modes appear as dictated by the center-manifold theorem. These are precisely the modes seen experimentally via the time-resolved Fourier transform (cf. above). There is of course no contradiction between the low dimensionality of the dynamics [Eqs. (7)] and the fact that many modes are seen in the field, since these are enslaved by the fundamental linearly unstable modes.

Finally, we want to reconstruct the phase diagram Fig. 1. As a first step we eliminate the trivial, fast time dependence that results from the periodic forcing. This is done by use of the two-time-scales method. One writes $\alpha_i(t) = \alpha_i^{(0)}(t,\tau) + \epsilon\alpha_i^{(1)}(t,\tau) + O(\epsilon^2)$, where $\tau = \epsilon t$ and $\epsilon = 2(\Omega_a - \Omega_b) \sim O(10^{-2})$. Inserting these definitions in Eqs. (7), equating terms of the same order of ϵ, and using the condition to remove secular terms, we arrive finally at the results $\alpha_a^{(0)} = a(\tau)e^{it/2}$, $\alpha_b^{(0)} = b(\tau)e^{it/2}$, and

$$\begin{aligned} da/d\tau &= (-La + i\phi_a)a + i\Gamma_1 a^* + i\Gamma_2|a|^2 a + i\Gamma_3|b^2|a + i\Gamma_4 a^* b^2, \\ db/dt &= (-L_b + i\phi_b)b + i\Delta_1 b^* + i\Delta_2|b|^2 b + i\Delta_3|a|^2 b + i\Delta_4 b^* a^2. \end{aligned} \tag{9}$$

Here Γ_i and Δ_i are γ_i/ϵ and δ_i/ϵ, respectively; $L_{a,b}$ are $\lambda_{a,b}/\epsilon$ and $\phi_{a,b} = (\Omega_{a,b} - \frac{1}{2})/\epsilon$. Equations (9) can be integrated numerically to explore the phase diagram. It turns out that the phase diagram of Fig. 1 is not fully reproduced. The asymmetry between the (4,3) and the (7,2) modes is observed but no chaotic behavior is found. This is not too surprising since the boundary condition $\partial\zeta/\partial n = 0$, on which we based our calculations, is not exact. However, the normal form and therefore the structure of Eqs. (9) is correct. We therefore base our further

TABLE I. Parameters used to reproduce the phase diagram.

$\omega_a = 49.4490\ \text{sec}^{-1}$	$\gamma_2 = -5.0\times10^{-3}$
$\omega_b = 50.2265\ \text{sec}^{-1}$	$\delta_2 = 6.5\times10^{-3}$
$\chi_a = 1.9249$	$\gamma_3 = \delta_3 = 8.5\times10^{-2}$
$\chi_b = 1.9684$	$\gamma_4 = \delta_4 = 0$
$L_a = L_b = 5\times10^{-4}/\epsilon$	$\gamma_1 = -\chi_a\Lambda/4\Omega_a$
	$\delta_1 = -\chi_b\Lambda/4\Omega_b$

analysis on these equations, treating the coefficients of the nonlinear terms as free parameters. The values of parameters used are displayed in Table I. We discuss here the part of the phase diagram in the close vicinity of the interesting point of intersection (which, strictly speaking, is also the range of validity of our theory). The results of the numerical investigation are shown in Fig. 3. The characteristics of Fig. 1 are reproduced: (i) the asymmetry between the modes, i.e., the fact that $f_{4,3}$ damps $f_{7,2}$, whereas $f_{7,2}$ pumps $f_{4,3}$; (ii) the existence of a region of periodic competition between the modes; and (iii) the existence of chaotic competition. Most importantly, the theory reproduces the fact that the boundaries between these regions converge close to the point of intersection, as seen experimentally. We note, however, that a careful search revealed periodic windows in the chaotic regime and also very small chaotic regions in the "periodic" regime, very close to the "boundary" with the chaotic regime. The slight disagreement with the frequency range between Figs. 1 and 3 is due to different boundary conditions. The variance in the values of A can be easily fixed by an adjustment of the parameters of Table I. We did not attempt to obtain a "best" fit.

To conclude, we have shown that one can go all the way from pde's to few-dimensional chaos in a hydrodynamic system of experimental interest. One can derive the nonlinear ode's including the coefficients. In fact, Eqs. (7), for either the modes (4,3) and (11,1) or (11,1) and (7,2) and with coefficients whose calculation is based on the formulas derived for the boundary condition $\partial\zeta/\partial n = 0$, should agree quite well with a similar experiment if done with a fluid that wets the walls efficiently. For the experiment at hand we could rationalize essentially all the major experimental findings. Further theoretical work will elucidate the mechanism for the transition to chaos in this system.

We are indebted to Ed Spiegel for useful conversations and to Jerry Gollub for sharing with us his results prior to publication and his insights. We thank Professor R. S. Berry and Professor L. P. Kadanoff for their wonderful hospitality at the University of Chicago. This work was supported by the Materials Research Laboratory of the University of Chicago, a National Science Foundation grant, and the Minerva Foundation, Munich, Germany.

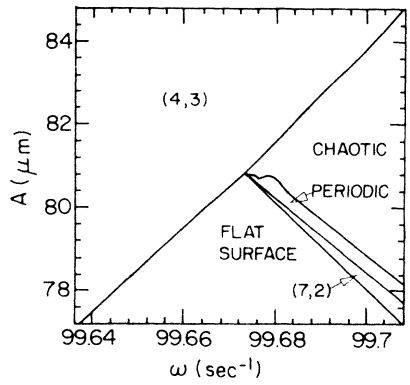

FIG. 3. The theoretical phase diagram. A is $2h|\Lambda|$.

[1]For recent reviews see N. B. Abraham, J. P. Gollub, and H. L. Swinney, Physica (Amsterdam) **11D**, 252 (1984); I. Procaccia, Phys. Scr. **T59**, 40 (1985), and references therein.

[2]Such a demonstration has been achieved in the context of mechanical systems. See P. Holmes and J. Marsden, Arch. Ration. Mech. Anal. **76**, 135 (1981); F. C. Mood and P. J. Holmes, J. Sound Vib. **65**, 275 (1979).

[3]S. Ciliberto and J. P. Gollub, Phys. Rev. Lett. **52**, 922 (1984), and J. Fluid Mech. (to be published).

[4]P. Coullet and E. A. Speigel, SIAM J. Appl. Math. **43**, 776 (1983).

[5]J. W. Miles, J. Fluid Mech. **146**, 285 (1984).

[6]T. B. Benjamin and F. Ursell, Proc. Roy. Soc. London, Ser. A **225**, 505 (1954).

[7]We were informed by S. Ciliberto that when the surface in the experiment becomes polluted (this influences the contact angles) a mode (11,1) could be seen between the (4,3) and (7,2) modes.

[8]John Guckenheimer and P. Holmes, *Nonlinear Oscillations, Dynamical Systems, and Bifurcations of Vector Fields* (Springer, New York, 1983).

[9]V. I. Arnold, *Geometrical Methods in the Theory of Ordinary Differential Equations* (Springer, New York, 1983).